International Journal of Mechanical Engineering and Research, ISSN 0973-4562 Vol. 5 No.1 (2015)

Design and Numerical Investigation of Static and Dynamic Loading Characters of Heterogeneous Model Leaf Spring

A. Sivasankar *(PG Scholar)*
Department of Mechanical Engineering (CAD/CAM)
RVS Technical Campus
Coimbatore, India.
sivasankar2411@gmail.com

Mr. B. Ramanathan *(Head of Department)*
Department of Automobile Engineering
RVS Technical Campus
Coimbatore, India.
ramanathan_pb@yahoo.com

***Abstract*- Suspension system is a major unit in automotive design, especially leaf spring design. It absorbs payload and road loads to give comfort to vehicle. Leaf spring system is an assembly, contains arched leafs put together by "U" bolts. Loads travel through each leaf and produce contact stress with each contact members, this effectively reduces the life time of the spring system. Spring steels are majorly preferred as leaf spring material, but in practical nature vehicle caries loads that are much higher than designed limit and causes earlier failure to leaf spring, which is a catastrophic in a driving condition and should be avoided. Preferring composite materials is very costly even though they are far better than metals, so, it is evident to develop an economical, maintenance friendly design for the leaf spring system. In this project work, a heterogeneous model leaf spring system is developed and numerically tested for a better suitability for the existing model. This model will introduce synthetic rubber sleeves between spring leafs, which is a hyperrealist material in nature, this system is designed and modeled through CAD software, dimensions and loading data are arrived from literature reviews. FEA based static and dynamic analysis will be conducted to study the behaviors of existing and heterogeneous models and the effectiveness of new model will be evaluated. The heterogeneous model is very economical alternative to many composite models proposed in the literature review and easy to manufacture, recyclable, and maintainable.**

I.INTRODUCTION

1.1 Suspension and Leaf Springs

Suspension can be considered as a link between the wheels and the body. It absorbs quick loadings and collects the elastic energy. Design fundamentals are based on the strength and comfort. The strength characteristics are usually determined according to the suspension type and loading. The comfort design fundamentals originate from the fluctuation and vibration point of view. The basic idea for the design is to generate the wanted elasticity and maintain the driving comfort. The leaf spring is one of the oldest suspension types. Nowadays it is widely used in heavy duty vehicles and work machines. Sometimes it is also called as a semi-elliptical spring; as it takes the form of a slender arc shaped length of spring steel (Fig.1.1) of rectangular cross section. The center of the arc provides the location for the axle, while the tie holes are provided at either end for attaching to the vehicle body. Supports the chassis weight, controls chassis roll more efficiently-high rear moment center and wide spring base, controls rear end wrap-up, controls axle damping, controls braking forces and regulates wheelbase lengths (rear steer) under acceleration and braking.

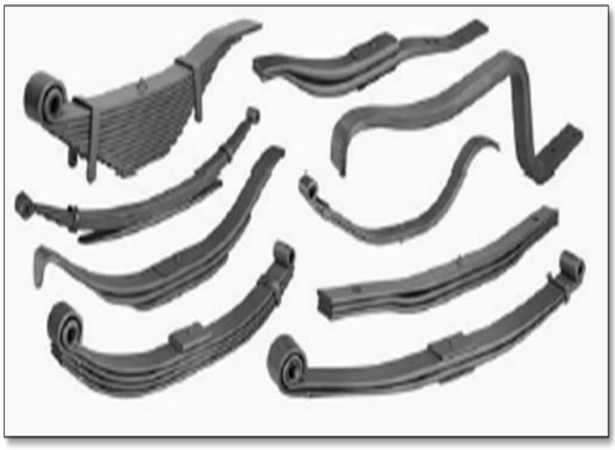

Fig1.1 - Leaf Springs

1.2 Simplified Model

In the cantilever beam type leaf spring (Fig.1.2), for the same leaf thickness, *h*, leaf of uniform width, *b* (case 1) and, leaf of width, which is uniformly reducing from *b* (case 2) is considered. From the basic equations of bending stress and deflection, the maximum stress σ_{max}, and tip deflection δ_{max}, can be derived. It is observed that instead of uniform width leaf, if a leaf of varying width is used, the bending stress at any cross section is same and equal to maximum stress σ_{max}. This is called as leaf of a uniform strength. Moreover, the tip deflection being more,

comparatively, it has greater resilience than its uniform width counterpart. Resilience, as we know, is the capacity to absorb potential energy during deformation.

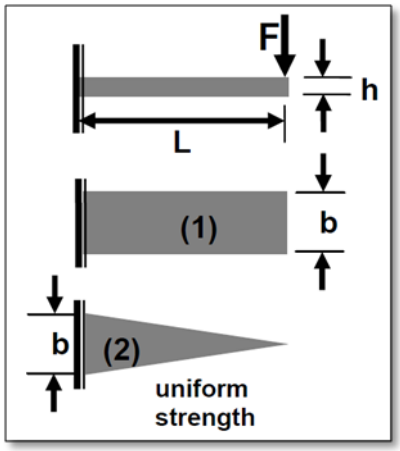

Fig1.2 - Beam Model with end point load

For Case (1) Uniform width and model as Fig.1.2

$$\sigma_{max} = 6FL/bh^2 \quad \text{(Eq.1.1)}$$

$$\delta max = 4FL^3/Ebh^3 \quad \text{(Eq.1.2)}$$

For Case (2) Non-uniform width and model as Fig.1.2

$$\sigma_{max} = 6FL/bh^2 \quad \text{(Eq.1.3)}$$

$$\delta max = 4FL^3/Ebh^3 \quad \text{(Eq.1.4)}$$

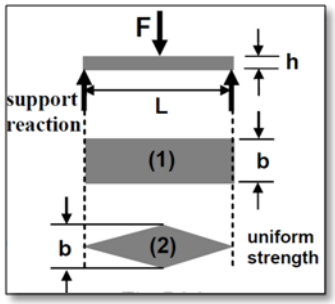

Fig 1.3 Beam Model with Midpoint load

For Case (1) Uniform width and model as Fig.1.3

$$\sigma_{max} = 3FL/bh^2 \quad \text{(Eq.1.5)}$$

$$\delta max = 2FL^3/Ebh^3 \quad \text{(Eq.1.6)}$$

For Case (2) Non-Uniform width and model as Fig.1.3

$$\sigma_{max} = 3FL/bh^2 \quad \text{(Eq.1.7)}$$

$$\delta max = 3FL^3/Ebh^3 \quad \text{(Eq.1.8)}$$

One of the applications of leaf spring of simply supported beam type (Fig.1.4) is seen in automobiles, where, the central location of the spring is fixed to the wheel axle. Therefore, the wheel exerts the force *F* on the spring and support reactions at the two ends of the spring come from the carriage.

Fig.1.4 Leaf Spring – Automotive

1.3 Design Foundation

Let us consider the simply supported leaf of Lozenge shape for which the maximum stress and maximum deflection are known. From the stress and deflection equations the thickness of the spring plate, *h*, can be obtained as,

$$h = \sigma_{max}. L^2 / E \delta_{max} = \sigma_{des}. L^2 / E \delta_{max} \quad \text{(Eq. 1.9)}$$

The σmax is replaced by design stress σdes similarly, σmax is replaced by σdes. *E* is the material property and depends on the type of spring material chosen. ***L*** is the characteristic length of the spring. Therefore, once the design parameters, given on the left side of the above equation, are fixed the value of plate thickness, ***h*** can be calculated. Substitution of ***h*** in the stress equation above will yield the value of plate width *b*.

$$b = 3\ FL / \sigma_{des}.h^2 \quad \text{(Eq. 1.10)}$$

In the similar manner h and b can be calculated for leaf springs of different support conditions and beam types.

1.4 Laminated Semi-Elliptic Spring

The figure 1.5 shows a laminated semi- elliptic spring. The top leaf is known as the master leaf. The eye is provided for attaching the spring with another machine member. The amount of bend that is given to the spring from the central line, passing through the eyes, is known as camber. The camber is provided so that even at the maximum load the deflected spring should not touch the machine member to which it is attached. The central clamp is required to hold the leaves of the spring.

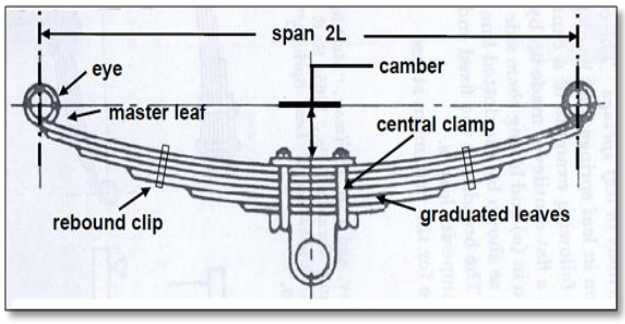

Fig.1.5 Laminated Leaf Spring

To prove that stress developed in the full length leaves is 50% more than that in the graduated leaves. The following steps should be performed.

1.5 Bending Stress and Displacement in the Graduated Leaves

For analysis half the spring can be considered as a cantilever. It is assumed that the individual leaves are separated and the master leaf placed at

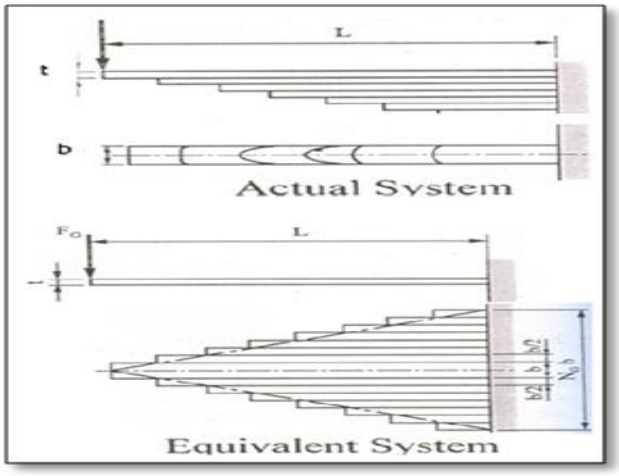

Fig.1.6 Actual and Equivalent Models

The center and then the second leaf is cut longitudinally into two halves, each of width (b/2) and placed on each side of the master leaf. A similar procedure is repeated for rest of the leaves the graduated leaves along with the master leaf thus can be treated as a triangular plate of thickness as shown in figure 1.6.

The bending stress developed in the graduated leafs will be as follows

$$\sigma_{bg} = 6F_gL / i_g bt^2 \qquad \text{(Eq. 1.11)}$$

For cantilever triangular plate, the deflection at the point of application of force is given by:

$$\delta_{g=} 6F_gL^3 / E\, i_g\, b\, t3 \qquad \text{(Eq. 1.12)}$$

1.6 Bending Stress and Displacements in Full Length Leaves

It is assumed that the individual leaves are separated and the full length leaf (Fig. 1.7) is placed at the center. Then the second full length leaf is cut longitudinally into two halves, each of width (b/2) and placed on each side of the first leaf. A similar procedure is repeated for the rest of the leaves.

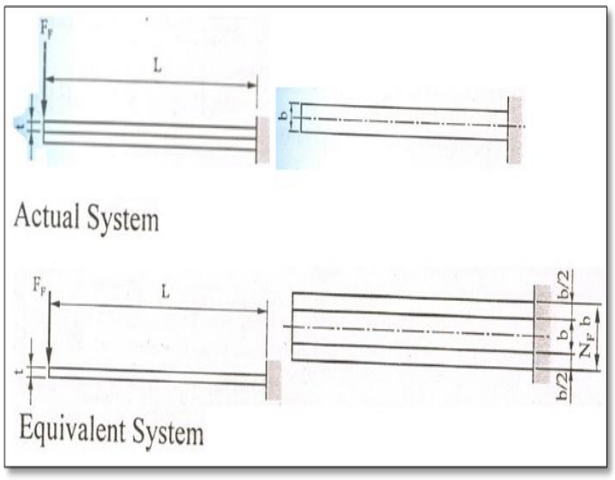

Fig. 1.7 Full Length Leaf

The bending stress developed in the full length leaves will be:

$$\sigma_{bf} = 6F_fL / i_f bt^2 \qquad \text{(Eq. 1.13)}$$

For a cantilever rectangular plate, the deflection at the point of application of force is given by:

$$\delta_{f=} 4F_lL^3 / E\, i_f\, b\, t3 \qquad \text{(Eq. 1.14)}$$

1.7 Solving Equation

$$\delta = \delta_g + \delta_f \qquad \text{(Eq. 1.15)}$$

Since the graduated leaves and the full leaves are clamped together the deflection for both should be the same.

$$F_g / F_f = 2i_g / 3\, i_f \qquad \text{(Eq. 1.16)}$$

$$F = F_g + F_f \qquad \text{(Eq.1. 17)}$$

$$F = F_f (1 + 2i_g / 3\, i_f) \qquad \text{(Eq. 1.18)}$$

Solving the above, we get

$$F_f = (3Fi_f / (3i_f + 2i_g)) \qquad \text{(Eq. 1.19)}$$

$$F_g = (3Fi_g / (3i_f + 2i_g)) \qquad \text{(Eq.1.20)}$$

Substituting the values of F_f and F_g in the equations of σ_{bf} and σ_{bg} we get;

$$\sigma_{bf=} 18\, FL / (3i_f + 2i_g)\, bt^2 \qquad \text{(Eq. 1.21)}$$

$$\sigma_{bg=} 12\, FL / (3i_f + 2i_g)\, bt^2 \qquad \text{(Eq. 1.22)}$$

Taking the ratios of both stresses and solving we get;

$$\sigma_{bf} / \sigma_{bg} = 1.5 \qquad \text{(Eq. 1.23)}$$

So the stress ratio between the full to the graduated is 1.5.The maximum deflection of the leaf spring can be found as follows; we have from previous equations, substituting any of the equation, Eq.14 or Eq.16 in Eq.15 or Eq.16.nConsider anyone of the deflection equation (Taking 6 and 12) and solving them we get.

$$\delta = 12\, FL^3 / (3i_f + 2i_g)\, Ebt^2 \qquad \text{(Eq. 1.24)}$$

1.8 Equalized Stress in Spring Leaves (Nipping)

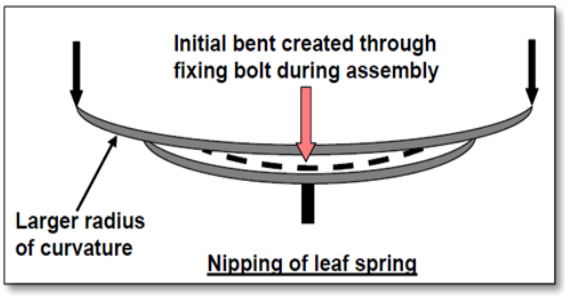

Fig 1.8 Nipping of Leaf Spring

- The stress in the full length leaves is 50% greater than the stress in the graduated leaves.
- To distribute this additional stress from the full length leaves, pre-stressing is done. This is achieved by bending the leaves to different radii of curvature, before they are assembled with the centre bolt
- The full length leaves are given in greater radii of curvature than the adjacent one. Due to the different radii of curvature, when the full length leaves are stacked with the graduated leaves, without bolting, a gap is observed between them. This gap is called Nip.
- The nip eliminated by tightening of the center bolt due to these pre-stresses is induced in the leaves. This method of pre-stressing by giving different radii of curvature is called as nipping.
- By giving a greater radius of curvature to the full length leaves than graduated leaves before the leaves are assembled to form a spring.

The value of the initial Nip ***C*** is nothing but the difference in deflection between the full length and the graduated leaves.

$$C = \delta g - \delta f \qquad = 2\,FL^3 / ibH^3E \quad \text{(Eq. 1.25)}$$

1.9 Spring Material Property

The most common leaf spring material used is silicon steel and the properties of the same if given below.

Name	: 65Si7 (Isotropic)
Young's modulus (E)	: 2.1e5 N/mm^2
Poisson's Ratio	: 0.266
BHN	: 400-425
UTS	: 1940 Mpa
Tensile strength Yield	: 1450 Mpa
Spring stiffness	: 221.5 N/mm^2
Density	: 7850 Kg/m^3

1.10 Mechanical Properties of Rubber

Rubber is a unique material that is both elastic and viscous. Rubber parts can therefore function as shock and vibration isolators and/or as dampers. Although the term *rubber* is used rather loosely, it usually refers to the compounded and vulcanized material. In the raw state it is referred to as an *elastomer*. Vulcanization forms chemical bonds between adjacent elastomer chains and subsequently imparts dimensional stability, strength, and resilience. An unvulcanized rubber lacks structural integrity and will "flow" over a period of time. Rubber mechanical properties as follows,

Hardness, shore A	: 10–90
Tensile strength	: 11 N/mm²
Elongation at break	: 100–1100%
Maximum temperature	: +300 °C
Minimum temperature	: -120 °C
E	: 9.70e5 N/mm²
Poisson Ratio	: 0.45

1.10.1 Rubber Compounding

Typical rubber compound formulations consist of 10 or more ingredients that are added to improve physical properties, affect vulcanization, prevent long-term deterioration, and improve process ability. These ingredients are given in amounts based on a total of 100 parts of the rubber.

1.10.2 Elastomer

Both natural and synthetic elastomer is available for compounding into rubber products. The American Society for Testing and Materials (ASTM) designation and composition of some common elastomers are shown in Table 1.1. Some elastomers such as natural rubber, Neoprene, and butyl rubber have high regularity in their backbone structure. They will align and crystallize when a strain is applied, with resulting high tensile properties. Other elastomers do not strain-crystallize and require the addition of reinforcing fillers to obtain adequate tensile strength. Natural rubber is widely used in shock and vibration isolators because of its high resilience (elasticity), high tensile and tear properties, and low cost. Synthetic elastomers have widely varying static and dynamic properties. Compared to natural rubber, some of them have much greater resistance to degradation from heat, oxidation, and hydrocarbon oils. Some, such as butyl rubber, have very low resilience at room temperature and are commonly used in applications requiring high vibration damping. The type of elastomeric used depends on the function of the part and the environment in which the part is placed. Some synthetic elastomers can function under conditions that would be extremely hostile to natural rubber.

Table 1.1 – ASTM Designation of Rubber

ASTM Designation	Common name	Chemical composition
N R	Natural rubber	cis-Polvisoprenc
I R	Synthetic rubber	cis- Polyisoprene
BR	Butadiene rubber	cis-Polyhutadiene
SBR	SBR	Poly (hutadiene-styrene)
II R	Butyl rubber	Poly (isohutylene-isoprene)
CuR	Chlorohutyl rubber	Chlorinated poly (isobutylene-isoprene)
B II R	Brornohutyl rubber	Brominated poly (isobutylene-isoprene)
EPM	EP rubber	Poly (ethylene-propylene)
EPDM	EPDM rubber	Poly (ethylene-propylene diene)
CSM	Flypalon	Chloro-sulfonyl-polyethylenc
CR	Neoprene	Poly chioroprene
NBR	Nitrile rubber	Poly (hutadiene-acrylonitrile)
HNBR	Hydrogenated nitrile rubber	Hydrogenated poiy(hutadienc-acrylonitrile)
ACM	Polyacrylate	Poly ethylacrylate
ANM	Polyacrylate	Poly (ethylacrylate
T	Polysulfide	Polysulfides
FKM	Fluoroelastorner	Poly fluoro compounds
FVMQ	Fluorosilicone	Fluoro-vinyl polysiloxane
MQ	Silicone rubber	Poly (dimethylsiloxane)
VMQ	Silicone rubber	Poly (methyiphenyl-siloxane)
PMQ	Silicone rubber	Poly (oxydirnethyl silylene)
PVMQ	Silicone rubber	Poly (polyoxymethylphenyl silylene)
AU	Urethane	Polyester urethane
EU	Urethane	Polyether urethane
GPO	Polyether	Poly (propylene oxide-allyl glycidyl ether)
CO	Epichlorohydrin homopolymer	Polyepichlorohydrin
ECO	Epichlorohydrin copolymer	Poly (epichiorohydrin-ethylene oxide)

An initial screening of potential elastomers can be made by determining the upper and lower temperature limit of the environment that the part will operate under. The elastomer must be stable at the upper temperature limit and maintain a given hardness at the lower limit. There is a large increase in hardness when approaching the *glass transition temperature.* Below this temperature the elastomer becomes a "glassy" solid that will fracture upon impact. Further screening can be done by determining the solvents and gases that the part will be in contact with during normal operation and the dynamic and static physical properties necessary for adequate performance.

1.10.3 Static Physical Properties

Rubber has properties that are drastically different from other engineering materials. Consequently, it has physical testing procedures that are unique.6 Rubber has both elastic and viscous properties. Which of these properties predominates frequently depends on the testing conditions.

1.10.4 Hardness

Hardness is defined as the resistance to indentation. The durometer is an instrument that measures the penetration of a stress-loaded metal sphere into the rubber. Hardness measurements in rubber are expressed in Shore A or Shore D units according to ASTM test procedures. Because of the viscoelastic nature of rubber, a durometer reading reaches a maximum value as soon as the metal sphere reaches maximum penetration into the specimen and then decreases the next 5 to 15 sec. Hand-held spring-loaded durometers are commonly used but are very subject to operator error. Bench-top dead-weight-loaded instruments reduce the error to a minimum.

1.10.5 Stress-Strain

Rubber is essentially an incompressible substance that deflects by changing shape rather than changing volume. It has a Poisson's ratio of approximately 0.5. At very low strains, the ratio of the resulting stress to the applied strain is a constant (Young's modulus).This value is the same whether the strain is applied in tension or compression. Hooke's law is therefore valid within this proportionality limit. However, as the strain increases, this linearity ceases, and Hooke's law is no longer applicable. Also the compression and tension stresses are then different. This is evident in load-deflection curves run on identical samples in compression, shear, torsion, tension, and buckling, as shown in Fig. 1.9 Rubber isolators and dampers are typically designed to utilize a combination of these

loadings. However, shear loading is most preferred since it provides an almost linear spring constant up to strains of about 200 percent. This linearity is constant with frequency for both small and large dynamic shear strains. The compression loading exhibits a nonlinear hardening at strains over 30 percent and is used where motion limiting is required. However, it is not recommended where energy storage is required. Tension-loading stores energy more efficiently than either compression-loading or shear-loading but is not recommended because of the resulting stress loads on the rubber-to-metal bond, which may cause premature failure. Buckled loading is a combination of tension- and compression-loading and derives some of the benefits of both.

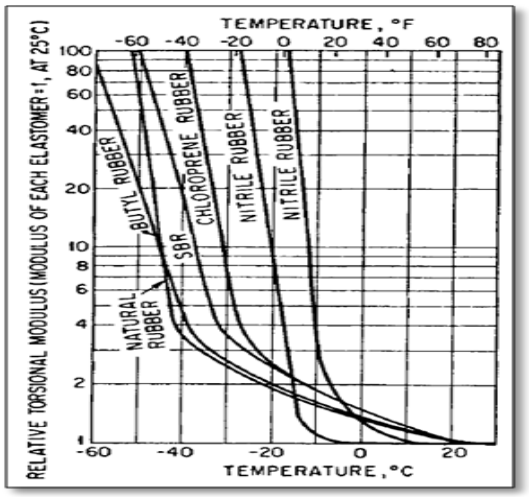

Fig 1.9 - Torsion modulus of elasticity Vs Temperature.

The stress-strain properties of rubber compounds are usually measured under tension as per ASTM procedures. Either molded rings or die-cut "dumbbell"-shaped specimens are used in testing. Stress measurements are made at a specified percentage of elongation and reported as modulus values. For example, 300 percent modulus is defined as the stress per unit cross sectional area (in psi or MPa units) at an elongation of 300 percent. Also measured are the stress at failure (tensile) and maximum percentage elongation. These are the most frequently reported physical properties of rubber compounds. The stiffness (spring rate) is the ratio of stress to strain expressed in Newton's per millimeter. It is dependent not only on the rubber's modulus but also on the shape of the specimen or part being tested. Since rubber is incompressible, compression in one direction results in extension in the other two directions, the effect of which is a bulging of the free sides. The *shape factor* is calculated by dividing one loaded area by the total free area.

1.10.6 Adhesion

Adequate rubber-to-metal adhesion is imperative in the fabrication of most vibration isolators and dampers. Adhesive is first applied to the metal; then the rubber is bonded to the metal during vulcanization. Various adhesives are available for all types of elastomers. In testing for adhesion, a strip of rubber is adhered to the face of a piece of adhesive-coated metal. After vulcanization (and possible aging), the rubber is pulled from the metal at an angle of 45° or 90°, and the adhesion strength is measured. The mode of failure is also recorded. Another ASTM method is used to determine the rubber-to-metal adhesion when the rubber is bonded after vulcanization, i.e., for post vulcanization bonding. In this procedure a vulcanized rubber disk is coated on both sides with an adhesive and assembled between two parallel metal plates. Then the assembly is heated under compression for a specified period of time. The metal plates are then pulled apart until rupture failure.

1.11 Finite Element Analysis

Traditional approach to design analysis involves the application of classical or analytical techniques. This approach has the following limitations:

1. Stresses and strains are obtained only at macro level. This may result in inappropriate deployment of materials. Micro level information is necessary to optimally allocate material to heavily stressed parts.
2. Adequate information will not be available on critically stressed parts of the components.
3. It may be necessary to make several simplifications and assumptions to design complex components and systems, if design analysis is carried out in the conventional manner.
4. Manual design is time consuming and prone to errors.
5. Design optimization is tedious and time consuming.

FEA is a convenient tool to analyze simple as well as complex structures. The use of finite element analysis is not restricted to mechanical engineering systems alone. FEA finds extensive application in electrical engineering, electronics engineering, micro electro mechanical systems, biomedical engineering etc. In manufacturing, FEA is used in simulation and optimization of manufacturing processes like casting, machining, plastic molding, forging, metal forming, heat treatment, welding etc. Structural, dynamic, thermal, magnetic potential and fluid flow problems can be handled with ease and accuracy using FEA. FEA was initially developed in 1943 by R. Courant to obtain approximate solution to vibration problems. Turner et al published in 1956 a paper on "Stiffness and Deflection of Complex Structures". This paper established a broader definition of numerical analysis as a basis of FEA. Initially, finite element analysis programs were mainly written for main frame and mini computers. With the advent of powerful PC's, the finite element analysis could be carried out with the help of several FEA software packages. Finite element method can be applied to a variety of design problems concerning automobiles, airplanes, missiles, ships, railway coaches and countless other engineering and consumer products.

1.12 General Steps Involved In Finite Element Analysis

1.12.1 Meshing or Discretization of Model

Finite element analysis looks at the model as a network of discrete interconnected elements. The Finite Element Method (FEM) predicts the behavior of the model by combining the information obtained from all elements making up the model. Meshing is a very crucial step in design analysis. The meshing is based on element size, tolerance, and local mesh control specifications. The mesh can be controlled for specify or different sizes of elements for components, faces, edges, and vertices. The software estimates a global element size for the model taking into consideration its volume, surface area, and other geometric details.

1.12.2 Solid Element

Linear elements are also called first-order, or lower-order elements. Parabolic elements are also called second-order, or higher-order elements. A linear tetrahedral element is defined by four corner nodes connected by six straight edges. A parabolic tetrahedral element is defined by four corner nodes, six mid-side nodes, and six edges. The following figures show schematic drawings of linear and parabolic tetrahedral solid elements.

Fig. 1.10 Element Types

In general, for the same mesh density (number of elements); parabolic elements yield better results than linear elements because: 1) they represent curved boundaries more accurately, and 2) they produce better mathematical approximations. However, parabolic elements require greater computational resources than linear elements. For structural problems, each node in a solid element has three degrees of freedom that represent the translations in three orthogonal directions. The software uses the X, Y, and Z directions of the global Cartesian coordinate system in formulating the problem.

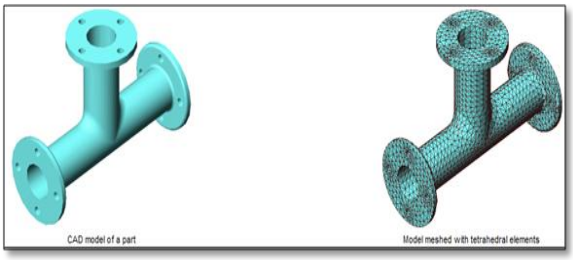

Fig. 1.11 Model and Meshed Model

1.12.3 Shell Element

A linear triangular shell element is defined by three corner nodes connected by three straight edges. A parabolic triangular element is defined by three corner nodes, three mid-side nodes, and three parabolic edges. For studies using sheet metals, the thickness of the shells is automatically extracted from the geometry of the model. Shell elements are 2D elements capable of resisting membrane and bending loads.

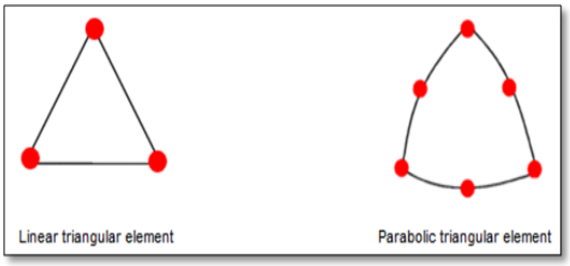

Fig. 1.12 Model and Meshed Model

For structural studies, each node in shell elements has six degrees of freedom; three translations and three rotations. The translational degrees of freedom are motions in the global X, Y, and Z directions. The rotational degrees of freedom are rotations about the global X, Y, and Z axes.

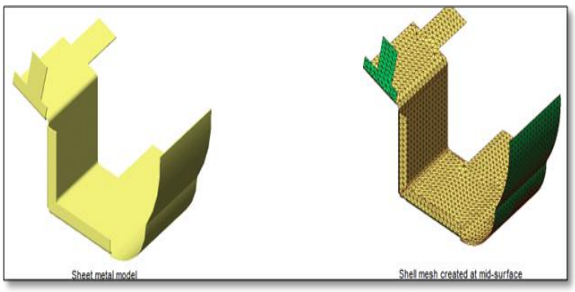

Fig. 1.13 Shell Meshed Model

1.12.4 Linear Static Analysis

When loads are applied to a body, the body deforms and the effect of loads is transmitted throughout the body. The external loads induce internal forces and reactions to render the body into a state of equilibrium. Linear Static analysis calculates displacements, strains, stresses, and reaction forces under the effect of applied loads.

Assumption in this type of analysis

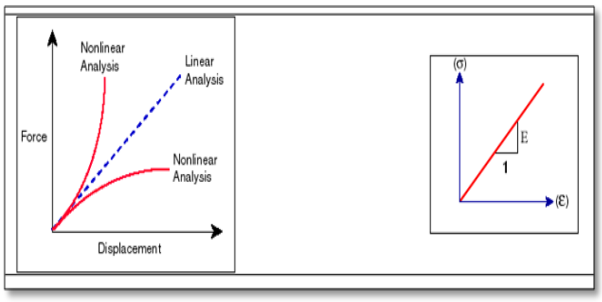

Fig. 1.14 Analysis Types in terms of Force Vs Displacement

1.12.5 Non-Linear Analysis

Linear static analysis assumes that the relationship between loads and the induced response is linear. All real structures behave nonlinearily in one way or another at some level of loading. In some cases, linear analysis may be adequate. In many other cases, the linear solution can produce erroneous results because the assumptions upon which it is based are violated. Nonlinearity can be caused by the material behavior, large displacements, and contact conditions.

1.12.6 Loads and Boundary Conditions

Loads and restraints are necessary to define the service environment of the model. The results of analysis directly depend on the specified loads and restraints. Loads and restraints are applied to geometric entities as features that are fully associative to geometry and automatically adjust to geometric changes.

The types of restraints are given below

Fixed: For solids this restraint type sets all translational degrees of freedom to zero. For shells and beams, it sets the translational and the rotational degrees of freedom to zero. For truss joints, it sets the translational degrees of freedom to zero. When using this restraint type, no reference geometry is needed

Roller/Sliding: Roller or Sliding restraint to specify that a planar face can move freely into its plane, but cannot move in the direction normal to its plane. The face can shrink or expand under loading.

Hinge: Hinge restraint to specify that a cylindrical face can only rotate about its own axis. The radius and the length of the cylindrical face remain constant under loading. This condition is similar to selecting the on cylindrical face restraint type and setting the radial and axial components to zero.

Symmetry: Symmetry type can be used to model a portion of the model instead of the full model. The results on the un-modeled portions are deducted from the modeled portion. When appropriate, taking advantage of symmetry can help you reduce the size of the problem and obtain more accurate results. The procedures to apply the symmetry restraint type to solid meshes and shell meshes using mid-surface are identical.

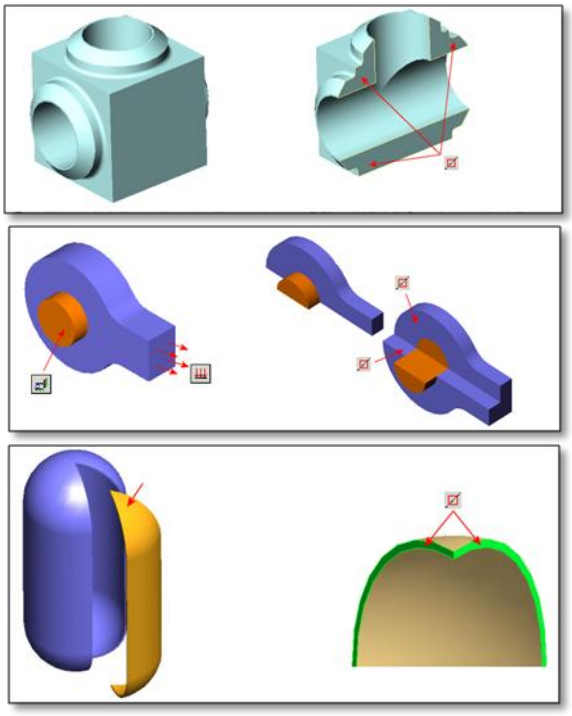

Fig. 1.15 Symmetry Model

Circular Symmetry: This allows you to analyze a model with circular patterns around an axis by modeling a representative segment. The segment can be a part or an assembly. The geometry, restraints, and loading conditions must be similar for all other segments making up the model. Turbine, fans, flywheels, and motor rotors can usually be analyzed using circular symmetry.

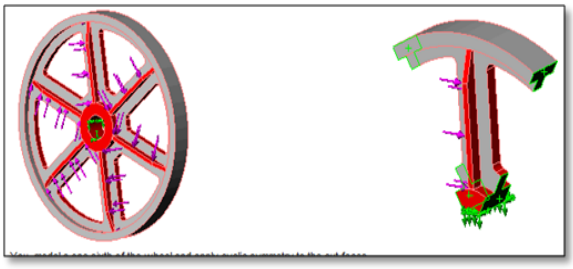

Fig. 1.16 Circular Symmetry

1.12.7 Types of Loads

Pressure, can be applied as uniform or non-uniform (variable) pressure to faces for use in structural (static, frequency, buckling, nonlinear and dynamic) analysis.

Table 1.2 Types of Loads – Pressure

		shells		the specified force to EACH entity.

Force, can be applied forces, moments, or torques with uniform distribution to faces, edges, reference points, vertices and beams in any direction for use in structural analysis.

Load Type		**Loaded Geometric Entities**	**Reference Geometry Entity**	**Required Input**
Normal Pressure	Uniform	Faces of solids and shells, and edges of shells	N/A	Unit and value of the pressure.
	Nonuniform	Faces of solids and shells, and edges of shells	Coordinate system to define distribution	Unit and value of the pressure and polynomial coefficients to define distribution.
Directional Pressure	Uniform	Faces of solids and shells, and edges of shells	Face, edge, or plane	Unit and pressure values in the desired direction.
	Nonuniform	Faces of solids and shells, and edges of shells	Face, edge, or plane for direction, and coordinate system for distribution	Unit and value of the pressure and polynomial coefficients to define distribution.

Table 1.3 Types of Loads - Force

Load Type		**Loaded Geometric Entities**	**Reference Geometry Entities**	**Required Input**
Normal Force	Uniform	Faces of solids and shells, and edges of	N/A	Unit and value of the force. The program applies
	Non-uniform	Faces	Coordinate system to define intensity	Unit and value of the force and polynomial coefficients to define the intensity. The program

				applies the specified force to EACH face.
Directional Force	Uniform	Reference points, vertices, edges, faces, joints, beams	Face, edge, plane, or axis	Unit and value of the force. The program applies the specified force to EACH entity.
	Nonuniform	Faces of solids and shells, edges of shells, beams	Face, edge, plane, or axis for direction, and a coordinate system for intensity	Unit and value of the force and polynomial coefficients to define the intensity. The program applies the specified force to EACH entity. Linear, parabolic, elliptical or table-driven distribution for beams
Torque		Faces (usually circular or cylindrical faces), beams.	Axis or a cylindrical face	Unit and value of the torque. The program applies the specified torque to EACH entity.

Gravity, this applies linear accelerations to a part or assembly document for use in structural and nonlinear analyses.

Table 1.4 Types of Loads - Gravity

Load Type	Loaded Geometric Entities	Reference Geometry Entity	Required Input
Gravity	Whole model	Face, edge, or plane	Unit and acceleration value. Material density must be defined.

II. LITERATURE REVIEW

Jawad A., et., al (2002) presented suspension system design for FSAE**.** The suspension system is one of the most important systems to consider when designing a FSAE car. All accelerations, either lateral or longitudinal, must be put to the ground through the tires, which are held in contact with the ground by the suspension system. The suspension system must therefore keep the largest contact tire patch at all times. If the suspension does a poor job of this, the car will not perform up to its full potential. A good suspension must therefore incorporate a good kinematics design to keep the tire as perpendicular to the pavement as possible, optimal damping and spring rates to keep the tire on the ground at all times, and strong components that do not deflect under the loads induced upon them. This suspension analysis is to be used as a guideline for future FSAE suspension teams. This suspension has been put through rigorous testing and has yet to fail on the 2002 Lawrence Technological University FSAE car. Each component has been improved through the years either made lighter or stronger with the use of computers, and finite element analysis (FEA).

Duni, et., al (2003), presented a numerical methodology based on the finite element method used for the transient dynamic simulation of the full vehicle rolling on different kind of obstacles. Some issues related to the tire finite element model development and its validation, by numerical experimental comparison, have been discussed. The strategy to combine the static simulations such as the tire inflating, the vehicle weight application and suspension pre loading, with transient dynamic analysis of the car rolling over the obstacle has been chosen. The methodology, based on integration of Abaqus Implicit and Explicit codes, has been successfully applied for the dynamic simulation of Fiat Punto car passing over comfort and pothole obstacle.

Aggarwala, et., al (2005) evaluated the axial fatigue strength of 65Si7 spring steel experimentally as a function of shot peening intensity for the application in the

automotive vehicles. Fatigue life at various shot peening conditions is determined with S/N curves and optimum shot peeling intensity is also determined. The effect of Almen intensity on compressive residual stress and relaxation of compressive residual stress have been discussed for fatigue life extension. Shot peening of leaf springs is illustrated to cause improvement in fatigue strength reduction in weight and reliability. A flow chart has been developed for improvement in fatigue design of components for economy.

Shankar S., et., al (2006) presents a low cost fabrication of complete mono composite leaf spring and mono composite leaf spring with bonded end joints. A single leaf with variable thickness and width for constant cross sectional area of unidirectional glass fiber reinforced plastic (GFRP) with similar mechanical and geometrical properties to the multileaf spring, was designed, fabricated (hand-layup technique) and tested. Computer algorithm using C-language has been used for the design of constant cross-section leaf spring. The results showed that a spring width decreases hyperbolically and thickness increases linearly from the spring eyes towards the axle seat. The finite element results using ANSYS software showing stresses and deflections were verified with analytical and experimental results. The design constraints were stresses (Tsai-Wu failure criterion) and displacement. Compared to the steel spring, the composite spring has stresses that are much lower, the natural frequency is higher and the spring weight is nearly 85 % lower with bonded end joint and with complete eye unit. Considering several types of vehicles that have leaf springs and different loading on them, various kinds of composite leaf spring have been developed. In multi-leaf composite leaf spring, the interleaf spring friction plays a spoil spot in damage tolerance. It has to be studied carefully. The following cross-sections of mono-leaf composite leaf spring for manufacturing easiness are considered. A) Constant thickness, constant width design, B) constant thickness, varying width design and C) varying width, varying thickness design. In this work, only a mono-leaf composite leaf spring with varying width and varying thickness is designed and manufactured. Computer algorithm using C-language has been used for the design of constant cross-section leaf spring. The results showed that a spring width decreases hyperbolically and thickness increases linearly from the spring eyes towards the axle seat. The wok provides the following results, the development of a composite mono leaf spring having constant cross sectional area, where the stress level at any station in the leaf spring is considered constant due to the parabolic type of the thickness of the spring, has proved to be very effective; the study demonstrated that composites can be used for leaf springs for light weight vehicles and meet the requirements, together with substantial weight savings; the 3-D modeling of both steel and composite leaf spring is done and analysed using ANSYS; a comparative study has been made between composite and steel leaf spring with respect to weight, cost and strength; the analytical results were compared with FEA and the results show good agreement with test results; from the results, it is observed that the composite leaf spring is lighter and more economical than the conventional steel spring with similar design specifications; adhesively bonded end joints enhance the performance of composite leaf spring for delamination and stress concentration at the end in compare with bolted joints.

SenthilKumar M. et., al (2007) presented static and fatigue analysis of steel leaf spring and composite multi leaf spring made up of glass fibre reinforced polymer using life data analysis. The dimensions of an existing conventional steel leaf spring of a light commercial vehicle are taken and are verified by design calculations. Static analysis of 2-D model of conventional leaf spring is also performed using ANSYS 7.1 and compared with experimental results. Same dimensions of conventional leaf spring are used to fabricate a composite multi leaf spring using E-glass/Epoxy unidirectional laminates. The load carrying capacity, stiffness and weight of composite leaf spring are compared with that of steel leaf spring analytically and experimentally. For this configuration maximum proof (bump) loading of the leaf spring is 3254 N, this value is taken for experimental, analytical and FEA analysis and all these were compared in this research work. The design constraints are stresses and deflections. Finite element analysis with full bump load on 3-D model of composite multi leaf spring is done using ANSYS 7.1 and the analytical results are compared with experimental results. Fatigue life of steel leaf spring and composite leaf is also predicted. Compared to steel spring, the composite leaf spring is found to have 67.35 % lesser stress, 64.95 % higher stiffness and 126.98 % higher natural frequency than that of existing steel leaf spring. A weight reduction of 68.15 % is also achieved by using composite leaf spring. It is also concluded that fatigue life of composite is more than that of conventional.

Lu Y., et., al (2009) carried out numerical simulation and field test are used to investigate tire dynamic load. Based on multi-body dynamics theory, a nonlinear virtual prototype model of heavy duty vehicle (DFL1250A9) is modeled. The geometric structural parameters of the vehicle system, the nonlinear characteristics of shock absorber and leaf springs are precisely described. The dynamic model is validated by testing the data, including vertical acceleration of driver seat, front wheel, intermediate wheel and rear wheel axle head. The agreement between the response of the virtual vehicle model and the measurements on the test vehicle is satisfactory. Using the reliable model, the effects of vehicle speed, load, road surface roughness and tire stiffness on tire dynamic load and dynamic load coefficient (DLC) are discussed. The results a road model of -30 mm to +30 for a distance of 1000m is formed for the standard *GB/T 7031-2005/ISO 8608.* This is used for the dynamic simulation. Virtual vehicle runs on the virtual road at constant speed of 60 km/h. The total simulation time and step size are 15 s

and 0.005, respectively. Vertical accelerations response of driver seat, front axle head, intermediate axle head and rear axle head are measured. The range of acceleration at front, intermediate and rear are -20K to +20K, -30K to 30 K and -30K to +25K. The observation of the road load at different speed with no load, half load and full load and with Class A, B, C and D road surfaces shows that the mid-axle experience a maximum load of 30KN at 60 Km/hr.

Cole, et., al (2010) presented, a research work concerned with measurement and simulation of the dynamic wheel loads generated by heavy vehicles. Dynamic wheel load data measured on an extensively instrumented articulated vehicle is used to validate a vehicle vibration simulation. The experimental data indicate that roll motions have some influence on the dynamic wheel loads at high frequencies, but do not influence the main low frequency force components due to sprung mass motion. Agreement between a pitch-plane simulation and experiment is good. The paper also describes a new "wheel load measuring mat" which can be used to measure the dynamic wheel loads generated by many uninstrumented vehicles. Preliminary test results indicate promising performance.

Kainulainen P, (2011), presented a fracture analysis for a parabolic leaf spring. The leaf spring type is used in a mining machine. The machine is designed for personnel and equipment transportation in a mine environment. The objectives were to gather information about effects of the improvement in the spring structure and study phenomena which eventually lead to the fracture of the spring. The project was divided into theoretical and experimental sections. The theoretical section included dynamic simulation with the multibody system approach and the finite element analysis. The multibody system was used to determine of the force flux of the spring. Values of the force flux were used as input forces in the finite element analysis. The experimental section consisted of strain gage measurements. Strain gage measurements were used to define stress levels in the examination point. The fatigue life time of the spring was calculated by using the loading history from measurements. The cause of the spring fracture was defined from results, produced by calculations and measurements. The results were also used as a criterion for the change of the spring type. As a final result, the project produced prototypes for new springs.

Sener A.S. et. al (2011) presented construction and standardization of a track for performing fatigue and reliability test of light commercial vehicles is described. For the design and process verification of the company's vehicles one test track is defined. A questionnaire was used to determine the average usage of light commercial vehicles in Turkey. Fatigue characteristics of Turkish roads were determined by analyzing fifty different roads and this article focuses on defining the load spectrum and equivalent fatigue damage of the leaf spring resulting from the accelerated test route. Fatigue analysis and estimated lifespan of the part were calculated using Finite Element Analyses and verified by the Palmgren-Miner rule. When the customer profile is taken into consideration; Turkish customer automotive usage profile, the aim of usage of this kind of vehicle (LCV), fatigue characteristics of Turkish roads for this vehicle were determined and around Bursa one accelerated test tracks were formed for the reliability and fatigue test for the related company, linear analysis executed on the FEA of the spring was more convenient were obtained.

Wu, et., al (2011) presented, vehicular axle load on top of a bridge deck is estimation including the effect of the road surface roughness which is modeled as a Gaussian random process represented by the Karhunen–Loève expansion. The bridge is modeled as a simply supported planar Euler–Bernoulli beam and the vehicle is modeled by a four degrees-of-freedom mass–spring system. A stochastic force identification algorithm is proposed in which the statistics of the moving interaction forces can be accurately identified from a set of samples of the random responses of the bridge deck. Numerical simulations are conducted in which the Gaussian assumption for the road surface roughness, the response statistics calculation and the stochastic force identification technique for the proposed bridge–vehicle interaction model are verified. Both the effect of the number of samples used and the effect of different road surface profiles on the accuracy of the proposed stochastic force identification algorithm are investigated. Results show that the Gaussian assumption for the road surface roughness is correct and the proposed algorithm is accurate and effective.

Harinath Gowd G. et. al (2012) carried out a work to analyze the safe load of the leaf spring, which will indicate the speed at which a comfortable speed and safe drive is possible. A typical leaf spring configuration of TATA-407 light commercial vehicle is chosen for study. Finite element analysis has been carried out to determine the safe stresses and pay loads. The work provides following conclusions, for safe and comfortable riding i.e., to prevent the road shocks from being transmitted to the vehicle components and to safeguard the occupants from road shocks it is necessary to determine the maximum safe load of a leaf spring. In the present work, leaf spring is modeled and static analysis is carried out by using ANSYS software and it is concluded that for the given specifications of the leaf spring, the maximum safe load is 7700N. It is observed that the maximum stress is developed at the inner side of the eye sections, so care must be taken in eye design and fabrication and material selection. The selected material must have good ductility, resilience and toughness to avoid sudden fracture for providing safety and comfort to the occupants.

Kadijk, et., al. (2012), presented a report on road load determination of passenger cars. Vehicle manufacturers typically determine the fuel consumption (in liters per 100

km) and CO2 emissions (in grammes per kilometer) in a test laboratory on a chassis dynamometer. In order to measure representative numbers this dynamometer must correctly simulate the vehicle resistance as function of the vehicle speed. This is performed on the basis of a measured road load curve. Before laboratory testing, determination of the vehicle road load curve takes place on a road or test track according to a legislative procedure. The result is a time-speed trace of the resistive load of the vehicle which must be simulated in the emission test on the chassis dynamometer. Within this project the main objective is to investigate for a number of vehicles whether the road load curves used for Type Approval testing are representative of commercially available production vehicles sold to customers. Road load curves of six modern passenger car models (Euro-5/Euro-6) and two older variants (Euro-4) of the same models have been determined on test tracks in The Netherlands and Belgium. The results have been compared to the road load settings used for Type Approval, (as specified by the manufacturer) and are expressed in a Road Load Ratio.

Kat J. (2012) presented validation of leaf spring model. In order to perform effective and reliable simulations in the CAE process, accurate simulation models of the vehicle and its associated systems, subsystems and components are required. In the vehicle dynamics context simulation models of the tyres, suspension, springs, damper, etc. are needed. This study will look at creating a validated model of a leaf spring suspension system used on commercial vehicles. The primary goal set for the model is to be able to predict the forces at the points where the suspension system is attached to the vehicle chassis as the model is to be used in full vehicle durability simulations. The component which will receive a considerable amount of attention in this study is the leaf spring. Leaf springs have been used in vehicle suspensions for many years. Even though leaf springs are frequently used in practice they still hold great challenges in creating accurate mathematical models. It is needless to say that an accurate model of a leaf spring is required if accurate full vehicle models are to be created.

Kumar Krishan, et., al (2012) carried out on a multi leaf spring having nine leaves used by a commercial vehicle. The finite element modelling and analysis of a multi leaf spring has been carried out. It includes two full length leaves in which one is with eyed ends and seven graduated length leaves. The material of the leaf spring is SUP9.The FE model of the leaf spring has been generated in CATIA V5 R17 and imported in ANSYS-11 for finite element analysis, which are most popular CAE tools. The FE analysis of the leaf spring has been performed by discretization of the model in infinite nodes and elements and refining them under defined boundary condition. Bending stress and deflection are the target results. A comparison of both i.e. experimental and FEA results have been done to conclude. The results shows when the leaf spring is fully loaded, a variation of 0.632 % in deflection is observed between the experimental and FEA result, and same in case of half load, which validates the model and analysis. On the other hand, bending stress in both the cases is also close to the experimental results. The maximum value of equivalent stresses is below the Yield Stress of the material that the design is safe from failure.

Mahesh J., et., al (2012), presented suitability of composite leaf spring on vehicles and their advantages. Efforts have been made to reduce the cost of composite leaf spring to that of steel leaf spring. The achievement of weight reduction with adequate improvement of mechanical properties has made composite a very replacement material for convectional steel. Material and manufacturing process are selected upon on the cost and strength factor. The design method is selected on the basis of mass production. From the comparative study, it is seen that the composite leaf spring are higher and more economical than convectional leaf spring. After prolonged use of conventional metal Coil Spring, its strength reduces and vehicle starts running back side down and also hits on the bump stoppers (i.e. Chassis). This problem is entirely removed by our special purpose Composite leaf Springs.

Peng, et., al (2012) presented a survey of graph theoretical approaches to image segmentation. Image segmentation is a fundamental problem in computer vision. Despite many years of research, general purpose image segmentation is still a very challenging task because segmentation is inherently ill-posed. Among different segmentation schemes, graph theoretical ones have several good features in practical applications. It explicitly organizes the image elements into mathematically sound structures, and makes the formulation of the problem more flexible and the computation more efficient. In this paper, we conduct a systematic survey of graph theoretical methods for image segmentation, where the problem is modeled in terms of partitioning a graph into several sub-graphs such that each of them represents a meaningful object of interest in the image. These methods are categorized into five classes under a uniform notation: the minimal spanning tree based methods, graph cut based methods with cost functions, graph cut based methods on Markov random field models, and the shortest path based methods and the other methods that do not belong to any of these classes. The present work motivates and details technical descriptions for each category of methods. The quantitative evaluation is carried by using five indices Probabilistic Rand (PR) index, Normalized Probabilistic Rand (NPR) index, Variation of Information (VI), Global Consistency Error (GCE) and Boundary Displacement Error (BDE) on some representative automatic and interactive segmentation methods.

Rahim A., et., al (2012) presented distributed fiber optic sensing: measuring strain along leaf spring. Leaf springs have many applications in the transportation

industry ranging from use in railway cars to vans and tractor-trailers. These components are widely used in commercial vehicles for their cost, simplicity, and their ability to spread weight over a larger area than a helical spring. While foil gages adhered to the spring will be able to provide strain information at various discrete points, utilizing fiber optic sensing allows the user to measure the strain profile across the entire length of the leaf spring with very high spatial resolution. Due to the fact that the strain profile along even a simple leaf spring is not uniform, distributed strain measurements provide a way to better characterize the effect of load on the spring. Fiber sensors are also able to handle the cyclic loading conditions present in suspension systems where foil gages often cannot.

KumarKrishan, et., al (2013) presented**,** Finite Element (FE) Analysis of mono steel leaf spring and a mono leaf spring made of composite materials i.e. Glass Reinforced Plastic (GRP) which is having high strength to weight ratio. The mono leaf spring is modeled with similar mechanical and geometrical properties to a conventional multi-leaf spring. The mono leaf spring model is having one full length leave with eyes at both ends & two pins in each eye end. The material of the mono steel leaf spring is SUP9. The CAE tools used for this work are CATIA V5 R17 for modeling & ANSYS-11 for FE Analysis. The FE analysis of leaf spring is performed for the deflection and stresses. In ANSYS, the general process of FEA is divided into three main phases i.e., preprocessor, solution, and postprocessor. The preprocessing of the model includes feeding various inputs like type of analysis, type of Element, Material properties, Geometric model, Meshing, Loading and boundary conditions. In Solution phase the FEA software generates element matrices, computes nodal values and derivatives in numerical form and stores the result data in files. The postprocessor phase is automatic which processes the result data and displays them in graphical form to check or analyze the result. A model of mono leaf spring of composite material, i.e. (GRP) is also prepared and analyzed by FE Analysis which is then compared with the previous mono steel leaf spring of. The use of composite materials resulted into reduction in deflection as well as in stresses. At the same time a large amount of material saving is also achieved by this material change.

Prasad K., et., al (2013), presented a work to predict the optimum design parameters using artificial neural networks. For this static and dynamic analysis on various leaf spring configuration is carried out by ANSYS and is used as training data for neural network. Training data includes cross section of the leaf, load on the leaf spring, stresses, displacement and natural frequencies. By creating a network using thickness and width of the leaf, load on the leaf spring as input parameters and stresses, displacement, natural frequencies as target data, stresses, displacement and natural frequencies can be predicted. By creating a network using values of stresses, displacement and load as input parameters to the network, thickness and width of the leaf spring as Target values, thickness and width of the leaf spring can be predicted. For independent values the two networks are tested and results are compared with the results obtained from ANSYS. Using PRO/E leaf spring was modeled and in ANSYS it was analyzed.

Ramakanth S., et., al (2013) carried out FE analysis approach for analysis of a multi leaf springs using Ansys software. The model is generated using solid works and imported in Ansys. The material of the leaf springs is 65Si7 (SUP9), composite leaf springs and hybrid leaf springs. Fatigue analysis of leaf springs is carried out for steel leaf springs, and Static analysis for steel leaf springs, composite leaf springs and hybrid leaf springs**.** Gradual loading from 1000N to 5000N were used in the analysis to find stress induced in the model and are presented. The stress level is in the order composite (GFRP) < Hybrid < Steel, weight reduction is in the order of steel 58.757kgs > Hybrid 41.41 kgs > composite 19.461kgs, cost comparison is in the order Composite >> Hybrid > Steel and fatigue analysis for steel shows better results with Soderberg's model.

2.1 Literature Review Findings for Static Structural Analysis

By studying the literature the following points were found for the present work.

1. Different type of leaf springs were taken for Static analysis
2. Analytical method is used for finding maximum bump load for conducting experimental and FEA simulation
3. Any standard leaf spring model can be designed, and its maximum static load can be found from the given literature review for FEA analysis
4. FEA methods for analysis were found with all boundary conditions and loadings

2.2 Literature Review Findings for Dynamic Structural Analysis

An acceleration range from -30 K to +30 K for a time period of 15 sec. with 0.005 as step is taken for analysis. Using Newton's second law (F=ma) we can find out the force vs time for the transient analysis. The data from the image of the acceleration Vs time chart is proposed to extract with the use of MATLAB and image processing algorithms.

III. PROBLEM DEFINITION AND PROPOSED SOLUTION

3.1 Problem Description

Leaf springs experience fluctuating loads with static loads of the vehicle and pay loads during its life time cycle. The springs were arranged in concentric arc model where each of them has contact at all loading conditions, the loads are transferred to the vehicle chassis through this contact load transfer, and this causes each leaf members experience the stress under all loading conditions. These leaf springs absorb road loads and shocks. While in riding, continuous change in the road surfaces bumps and pot holes make fluctuation loads in the spring members, this decrease service life of the spring members and in turn the whole system. Minimization of the load absorption between leaf members or minimize contact will increase the life. But, the cost of the new or modified system must be an economical one and in terms of maintenance and replacement. So, there is a strong need for a new and innovative economical stress minimization system.

3.2 Proposed Solution

It is clear that, minimizing contact loading will yield improvement in the service life of the leaf spring system. The literature reviews provides enough guidance in leaf spring dimensional details, static loading details from experiment and finite element analysis. Most of the authors proposed composite material model as a better alternate for the leaf spring system, even though it has advantages in strength and fatigue life, it is nerve an economical model for vehicles in the present situation, more over the manufacturing and serviceability is difficult for them. Considering all these factors, a Hyperelastic material (Synthetic Rubber) as an interleaf between leaf springs is proposed in this project work. Rubber can elongate several hundred times than its original shape and retain the same after loading, this behavior is called Hyperelastic, by introducing this Hyperelastic material between leaf spring members will absorb the loads and stress due them. The behaviors of this proposed heterogeneous model will be evaluated through static and dynamic analysis and compared with the existing model.

IV. METHODOLOGY

4.1 Methodology Description

The methodology provides a systematic approach to the project work, it begins from the objective formulation and end with final phase proceedings the following diagram shows the methodology. Each stage provides the necessary details to carry out the project work; literature review is the key element in the diagram where, the objective gets in to problem formulation and proposed solution phase. The next stage is branched into static and dynamic analysis, which leads to result and discussion stage followed by final phase progress details.

4.2 Design Details

This section provides the basic design procedure for the design of leaf springs. Based on inputs the design is performed.

4.3 Design Procedure

Let the deflection of the beam is as follows

$$\delta = (f L^2) / (4 E t) \quad \text{(Eq.4.1)}$$

$$f = (3 P L) / (2 bt^2 n) \quad \text{(Eq.4.2)}$$

Substituting value of f from Eq.6.2 in Eq. 6.1, results the following.

$$\delta = (3 P L^3) / (8 Enbt^3) \quad \text{(Eq.4.3)}$$

When extra full is added the Eq.5.3 is became

$$\delta = (f L^2) / 2 (2 + k) E t \quad \text{(Eq.4.4)}$$

Where

P=Maximum load on the spring (N)
n=Number of leaves
L=Length of the spring (mm)
t=Thickness of the leaves (mm)
b=Width of the leaves (mm)
f =Maximum Stress (N/mm^2)
δ=Deflection or camber of the spring (mm)
n_1=Number of extra full length leaves
n=Total number of leaves
n_f=Number of full leaves
n_g=Number of graduated leaves
x=U –Bolt Distance (mm)
L=Total length of spring
$k = n_1 / n$

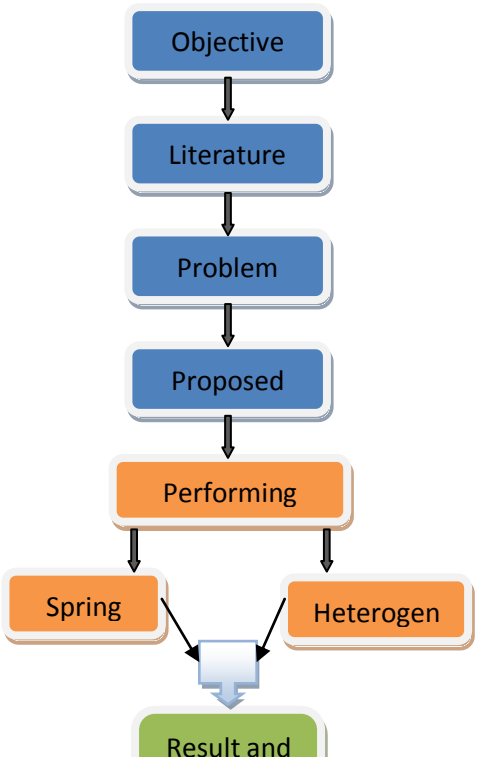

Fig. 4.1- Methodology

The following table shows the standard width and thickness prescribed by IS 3431-1965.

Table 4.1 – IS 3431-1965

Width (mm)	40	45	50	55	60	65	70	90	100
Thickness (mm)	4	5	6	7	8	10	12	14	16

4.4 Eye Diameter

d = Eye diameter (mm)
l = Length of the pin (mm)
f_b = Bearing Stress (N/mm^2)
ld = Area under bearing (mm^2)

$$d = P / (f_b \, l \cos 45) \quad \text{(Eq. 4.5)}$$

The pin can be checked for shear

$$f_s = (P \, 2 \sqrt{2}) / (\pi d^2) \quad \text{(Eq. 4.6)}$$

fs < f (for design safe)

4.5 Length of Graduated Leafs

If $n_f = 1$, then the number of leaf to be cut is *n* and if $n_f = 2$ the number of leaves to be cut is (n -1) and two of full length leaves will be of small length (including master leaf).

Length of the smallest leaf

$$L1 = L / (n - 1) + x \quad \text{(Eq. 4.7)}$$

Length of the second graduate leaf

$$L2 = (L / (n - 1)) \, 2 + x \quad \text{(Eq. 4.8)}$$

For 3, 4, 5 (up to the number of graduated leaf count)

$$L3 = (L / (n - 1)) \, 3 + x \quad \text{(Eq. 4.9)}$$

$$L4 = (L / (n - 1)) \, 4 + x \quad \text{(Eq. 4.10)}$$

$$L5 = (L / (n - 1)) \, 5 + x \quad \text{(Eq. 4.11)}$$

Master leaf length

Lm=Length of Master leaf + Allowance for eye

$$Lm = L + 2\pi (d + t) \quad \text{(Eq. 4.12)}$$

4.6 Model

The following figures show the solid models of the leaf spring system that is taken for the analysis. The model dimensions are taken from the literature review [5].and tested with the given condition and compared with the experimental results. Since the eye diameter and U-bolt dimensions are not specified in any of the literature review, the FEA results may vary ± 10% from the actual.

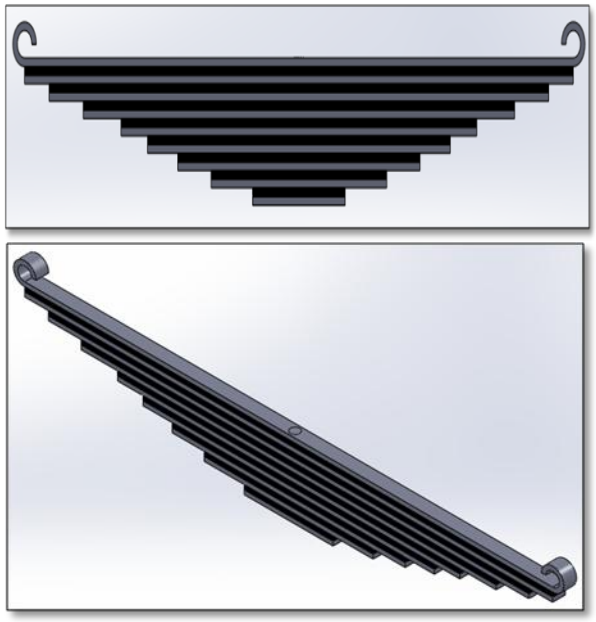

Fig 4.2 – Heterogeneous Model (Rubber Interleafs)

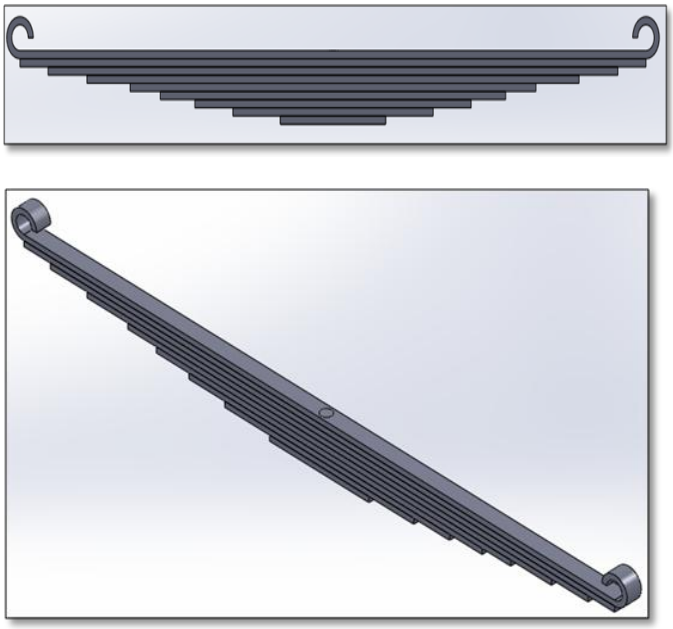

Fig 4.3 – Actual Model

4.7 Simulation Parameters

4.7.1 Leaf Dimension

Length of full length leaves (L-1 and L-2) : 1450mm each
Width of all leaves : 70mm
Thickness of all leaves : 12mm
No. of extra full length leaf : 1
Number of graduated length leaves : 07
(L-3, L-4, L-5, L-6, L-7, L-8 and L-9) :
1320,1140,940, 800,640,464,244 mm

4.7.2 Boundary Conditions

The eyes of the leaf springs are fixed and a static loading of 35000 N, will be applied for static analysis.

4.7.3 Static Analysis

The following figure shows the imported model of the leaf spring assembly for perfoaming static analysis.

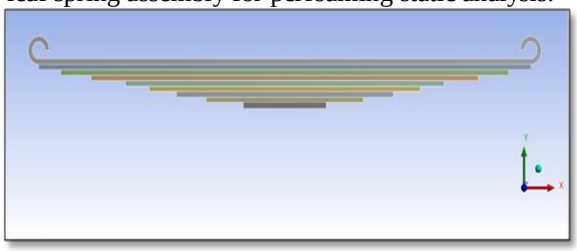

Fig. 4.4 - Leaf Spring Assembly

The assembly contains 9 leafs, two of them are master leafs and other seven are graduated leafs.

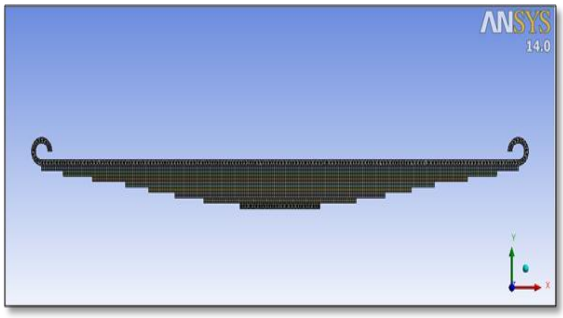

Fig 4.5 – Mesh

The above figure shows the meshed model of the leaf assembly. It contains 193313 nodes and 47666 elements made of tetra and Hexa type 3d elements. The following figure shows the boundary condition. The master leaf eyes are fixed.

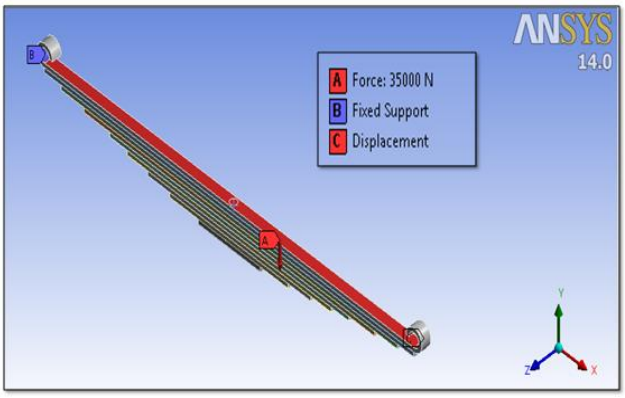

Fig. 4.6 - Boundary Condition

The following figure shows the loading condition of the model, the static loading of 35000 N is applied on the master leaf spring.

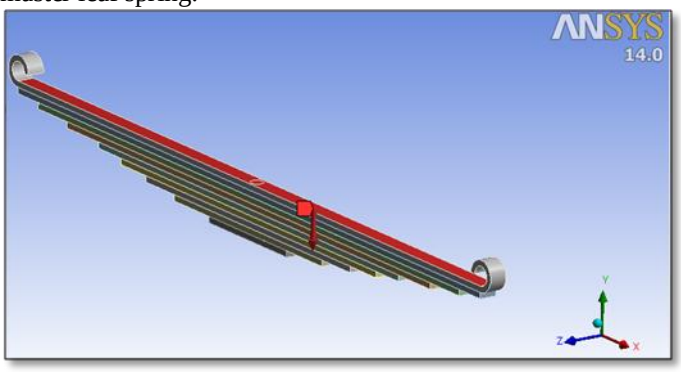

Fig. 4.7 - Loading Condition

The static loading condition is arrived from the literature reviews, for the same model the load is applied at the master's leaf's top face. When the model is taken cambered the load must be applied at the bottom leaf to simulate the real situation. Here the un-cambered model is taken and applied at the top. The following figure show the maximum deflection that the leaf assembly experience under static loading condition. The maximum value is 156.85 (153 + 3.85) mm.

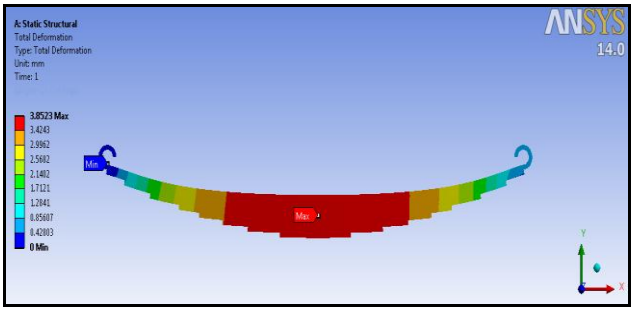

Fig. 4.8- Total Deformation

The following figure shows the VonMises stress of the leaf assembly, it is maximum (1054.1 Mpa) at the leaf eyes and it is understandably so, because of the one fixed and one movable ends.

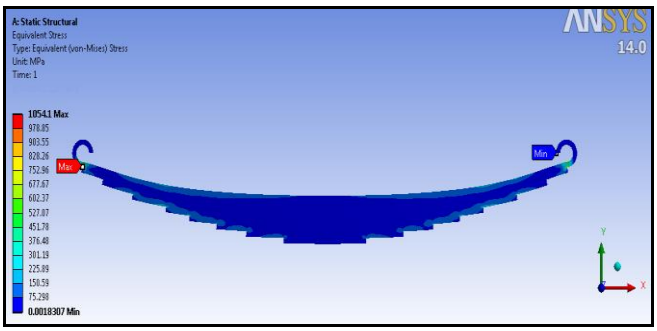

Fig. 4.9 - VonMises Stress

The Tensile stress of the spring material is 1470 Mpa which is much higher than the induced VonMises stress.

4.8 Heterogeneous Model Analysis

The following figure shows the heterogeneous model, the model consists of 9 steel leafs, which are interleafed with synthetic rubber. The thickness of the rubber sleeves are same thickness (12 mm) as steel leafs.

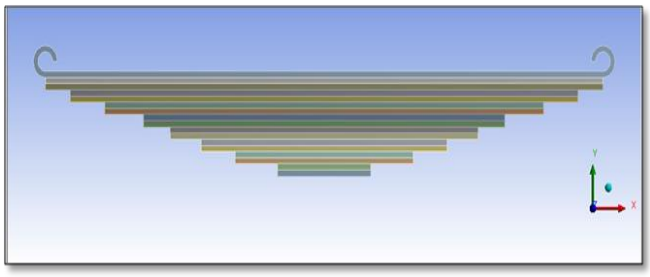

Fig. 4.10 – Heterogeneous Model

The following figure shows the meshed model, contains 101616 nodes and 118608 elements.

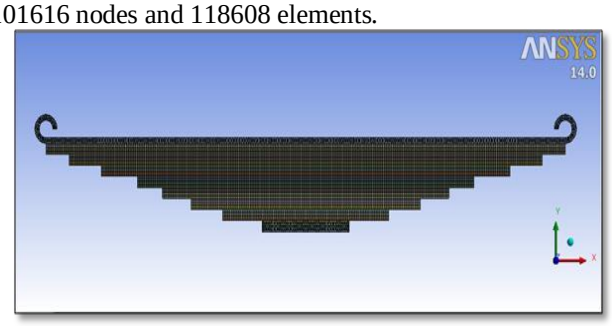

Fig. 4.11 – Meshed Model

4.9 Boundary Condition

The following figure shows the boundary condition, fixed ends and loading of 35000 N.

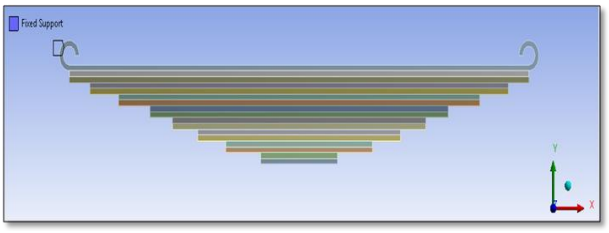

Fig. 4.12 – Fixed Eye

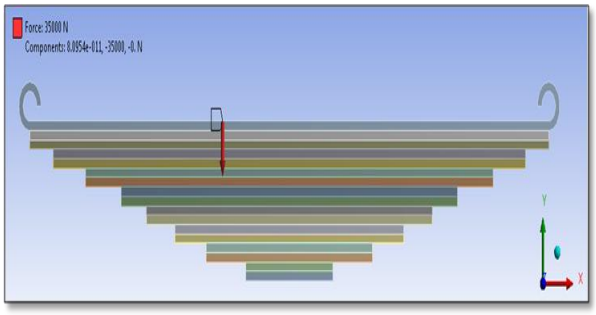

Fig. 4.13 – Loading

4.10 Results

The following figure shows the VonMises stress. The maximum value shows 146.30 Mpa.

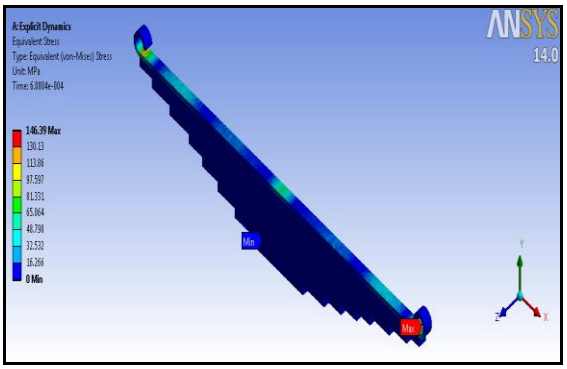

Fig. 4.14 – VonMises Stress

The following figure shows the maximum shear stress in the model. The value shows 77.722 Mpa.

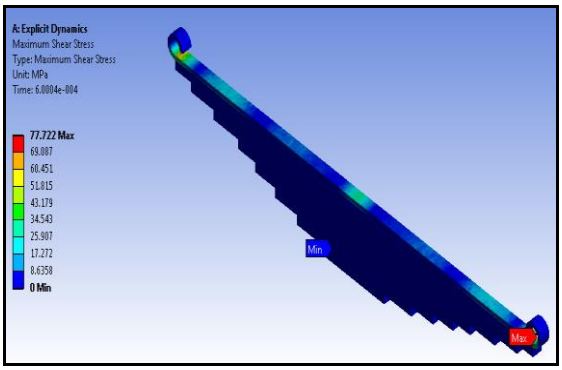

Fig. 4.15 – Shear Stress

V. RESULT AND DISCUSSION

5.1 Static Analysis

The static analysis of the steel leaf model shows the following results

Table 5.1 – Results Comparison

Description	Experimental [5]	FEA	% Difference
Load (N)	35000	35000	0
Max. Stress (Mpa)	1018.00	1054.1	+ 10
Deflection (mm)	158.00	156.85	0.7

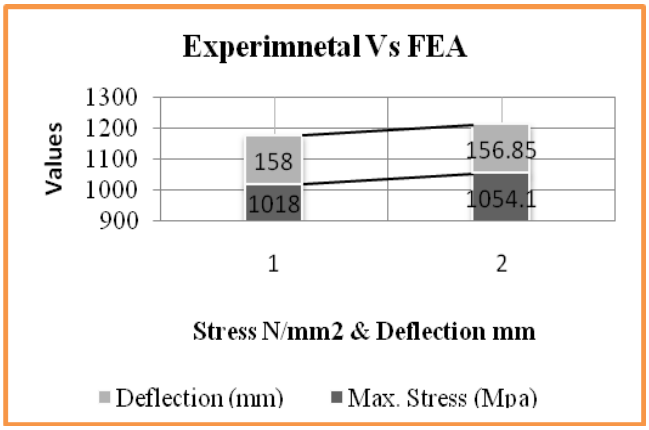

Fig. 5.1 – Static Analysis - Results

The result shows that the value gives acceptable nearer results to the experimental result.

5.2 Heterogeneous Model Static Analysis

The following table shows the comparison results of the normal steel and heterogeneous model.

Table 5.2 – Result Comparison - 2

Description	Steel	Heterogeneous	% Reduction
Load (N)	35000	35000	0
Max. Stress (Mpa)	1054	146.30	86.15

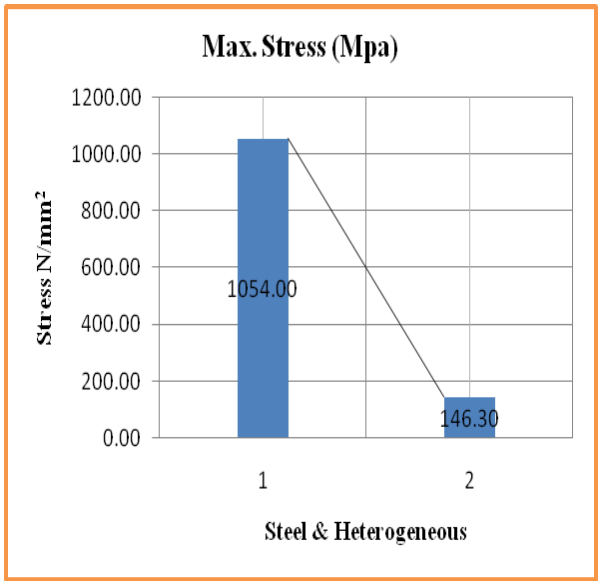

Fig. 5.2 – Heterogeneous Model Static Analysis

5.3 Discussion

Static analysis of existing and heterogeneous models of leaf springs was numerically investigated and the results show better correlation. The existing model shows 18% deviation with experimental stress value, it can be further investigated with refined mesh technology.

The implementation of heterogeneous model in the form of silicon rubber leafs between existing leaf provides best result in reducing the stress, the inter rubber leafs absorbs around 86% of actual stress due to static loading. This shows the implementation will definitely yield a better alternate for the existing steel only model or any other high cost composite models that were discussed in the literatures

The present work concludes that the heterogeneous is far better alternate to high cost composite and existing steel-only model leaf spring and effectively reduces the stress (86%) in the leaf assembly, which will increase life of the same.

In the final phase of the project work, transient analysis of the heterogeneous model and spring steel model will be performed for the given load vs. time data, which is evaluated from images acquired from experimental investigations as an acceleration vs. time graph in the form of signals, the data is referred from literature review.

Since the data is in image form with signals it is necessary to get data of the time and acceleration in numerical format to do so image-processing technique will be employed through MATLAB software.

Using this renewed tool, the time vs acceleration can be extracted from the signal image and them applying Newton's second law the time vs force plot will be generated. The same will be used for performing transient analysis to predict the stress strain behaviors of the leaf spring models.

VI. REFERENCES

[1] Aggarwala (2005) et, al 'Influence of shot preening intensity on fatigue design reliability of 65Si7 spring steel', IJE&MS.
[2] Badih A. (2002) et. al ' Design of Formula SAE Suspension', ISSN 0148-7191, SAE International.
[3] Cole D.J. (2010) et. al 'Simulation And Measurement Of Dynamic Tyre Forces', Vehicles and Environment Division of the Transport and Road Research Laboratory (TRRL), UK and by Golden River Ltd.
[4] Duni E. (2003) et. al 'Numerical Simulation Of Full Vehicle Dynamic Behavior Based On The Interaction Between Abaqus/Standard And Explicit Codes'. ABAQUS Users' Conference.
[5] Harinath G. Gowd et. al (2012) 'Static Analysis Of Leaf Spring", International Journal of Engineering Science and Technology (IJEST), ISSN : 0975-5462 Vol. 4 No.08.
[6] Kadijk G. (2012) 'Road load determination of passenger cars', Behavioural and Societal Sciences, VanMourik Broekmanweg, Delft, The Netherlands.
[7] Kainulainen (2011) "Analysis of Parabolic Leaf Spring Failure", Thesis, University of Applied Science.
[8] Kat J. (2012), "Validated Leaf Spring suspension models", Thesis.
[9] Krishan K. et. Al (2012) 'A Finite Element Approach for Analysis of a Multi Leaf Spring using CAE Tools', Research Journal of Recent Sciences ISSN 2277-2502 Vol. 1(2), pg 92-96.
[10] Krishan K. (2013) et. al 'Computer Aided Fea Comparison Of Mono Steel And Mono Grp Leaf Spring'. International Journal of Advanced Engineering Research and Studies, E-ISSN2249–8974.
[11] Lu Y. (2010) et. al 'Numerical and experimental investigation on stochastic dynamic load of a heavy duty vehicle', Applied Mathematical Modeling, 34 2698–2710, Elsevier Inc.
[12] Mahesh J. (2012) et. al, 'Performance Analysis of Two Mono Leaf Spring Used For Maruti 800 Vehicle', International Journal of Innovative Technology and Exploring Engineering (IJITEE) ISSN: 2278-3075 Vol-2, Issue-1.
[13] Mouleeswaran et. Al (2007) 'Analytical and Experimental Studies on Fatigue Life Prediction of Steel and Composite Multi-leaf Spring for Light Passenger Vehicles Using Life Data Analysis', ISSN 1392–1320 Materials Science (MEDŽIAGOTYRA). Vol. 13, No. 2.
[14] Penga B (2005) 'A Survey of Graph Theoretical Approaches to Image Segmentation'. SPIE, 5665: pp 288– 299.
[15] Prasad K. (2003) et. al 'Prediction Of Leaf Spring Parameters Using Artificial Neural Networks', International Journal of Engineering Science and Technology (IJEST) Vol 2, pp 257-268.
[16] Rahim A. (2012) et. al 'Superior Fatigue Characteristics of Fiber Optic Strain Sensors', In Aircraft Structural Integrity Program Conference.
[17] Ramakanth U. S. et. al (2013) ' Design And Analysis Of Automotive Multi-Leaf Springs Using Composite Materials', International Journal of Mechanical Production Engineering Research and Development (IJMPERD), ISSN 2249-6890. Vol. 3, Issue 1, pg 155-162.
[18] Sener A.S. (1998) et. al, 'Determination Of Vehicle Components Fatigue Life Based On FEA Method And Experimental Analysis', International Journal Of Electronics, Mechanical And Mechatronics Engineering Vol.2 Num.1, pp. (133-145).
[19] Siddaramanna G. (2006) et. al 'Mono Composite Leaf Spring for Light Weight Vehicle Design, End Joint Analysis and Testing', ISSN 1392–1320, Materials Science (MEDŽIAGOTYRA). Vol. 12, No. 3.
[20] Wu S.Q (2011) et. al 'Vehicle axle load identification on bridge deck with irregular road surface profile', Engineering Structures 33, pp 591–601, Elsevier Ltd.